Spectrochimica Acta Part B 63 (2008) 652–656

Contents lists available at ScienceDirect

Spectrochimica Acta Part B

journal homepage: www.elsevier.com/locate/sab

Foreign gas broadening and shift of the strongly "forbidden" lead line at 1278.9 nm

Vlasta Horvatic [a,*], Damir Veza [b], Mladen Movre [a], Kay Niemax [c], Cedomil Vadla [a]

[a] Institute of Physics, Bijenicka 46, 10000 Zagreb, Croatia
[b] Department of Physics, Faculty of Science, University of Zagreb, Bijenicka 32, 10000 Zagreb, Croatia
[c] ISAS-Institute for Analytical Sciences at the Technical University of Dortmund, Bunsen-Kirchoff-Str. 11, D-44139, Dortmund, Germany

ARTICLE INFO

Article history:
Received 15 February 2008
Accepted 9 April 2008
Available online 18 April 2008

Keywords:
Broadening rate
Shift rate
Lead
Forbidden transition

ABSTRACT

The collisional broadening and shift rate coefficients of the "forbidden" $6p^2\ ^3P_0 \rightarrow 6p^2\ ^3P_1$ transition in lead were determined by diode laser absorption measurements performed simultaneously in two resistively heated hot-pipes. One hot-pipe contained Pb vapor and noble gas (Ar or He) at low pressure, while the other was filled with Pb and noble gas at variable pressure. The measurements were performed at temperatures of 1220 K and 1290 K, i.e., lead number densities of 4.8×10^{15} cm^{-3} and 1.2×10^{16} cm^{-3}. The broadening rates were obtained by fitting the experimental collisionally broadened absorption line shapes to theoretical Voigt profiles. The shift rates were determined by measuring the difference between the peak absorption positions in the spectra measured simultaneously in the heat pipe filled with noble gas at reference pressure and the one with noble gas at variable pressure. The following data for the broadening and shift rate coefficients due to collisions with Ar and He were obtained: $\gamma_B^{Ar}=(3.4\pm0.1)\times10^{-10}$ cm^3 s^{-1}, $\gamma_B^{He}=(3.8\pm0.1)\times10^{-10}$ cm^3 s^{-1}, $\gamma_S^{Ar}=(-7.3\pm0.8)\times10^{-11}$ cm^3 s^{-1}, $\gamma_S^{He}=(-6.5\pm0.7)\times10^{-11}$ cm^3 s^{-1}.

1. Introduction

The broadening and shift of atomic spectral lines by collisions with neutral atoms has been studied extensively since the very beginning of atomic physics [1–3]. These studies provide insight into the nature of interatomic forces and, hence, they provide an excellent test of theory. Careful analysis of line profiles is a powerful technique for studying atomic and molecular interactions and is often necessary for probing matter in extreme conditions, such as in stellar atmospheres [4], ultracold traps and Bose–Einstein condensates [5]. The collisional broadening and shift coefficients are useful for plasma diagnostics and analysis of emission from gaseous discharges. Further, collisional line broadening also provides an optical bandwidth control method for ultra-narrow-band atomic filters [6]. The collisional broadening rate coefficients find frequent application in the determination of various physical quantities, e. g., transition oscillator strengths [7] or cross sections for certain excitation energy transfer reaction [8–13]. Knowledge about atom number density of the investigated gaseous medium is often required to determine such quantities, and when this is done by spectroscopic means by analyzing collisionally broadened line profile [14–16], the broadening rate coefficients are the parameters that are requisite for the evaluation of the results.

A review of early experimental work in the field of foreign gas broadening was given by Chen and Takeo [2]. A survey of more recent results can be found in [3], while a comprehensive bibliography of theoretical and experimental papers published in the period from 1978 to 1992 is available from NIST [17]. To date a great deal of studies were concerned with rare-gas broadening, especially of the alkalis, but small number of papers were reported on heavier elements such as lead. Available data concern the noble gas (Ar, He) broadening and shift of the lead resonance line at 283.39 nm [15,18], and three lines (364.06, 368.45 and 405.90 nm) belonging to the multiplet transition between metastable $6p^2\ ^3P_{J'}$ and $7s\ ^3P_J^0$ state (see Fig. 1a). To our knowledge, broadening and shift of the strongly "forbidden" lead lines (938.9 and 1278.9 nm) occurring in the $6p^2\ ^3P_0 \rightarrow 6p^2\ ^3P_J$ transitions between the ground and metastable states have not yet been investigated. In the present paper we report the broadening and shift rates of the 1278.9 nm Pb line (Fig. 1b) induced by collisions with Ar and He. These data can find its application in the development of spectrochemical techniques for the analysis of heavy elements in low-pressure noble gas discharges, where they are needed in the process of modeling and optimization of the conditions in the discharge [16].

2. Experiment

The experimental setup used in the present experiment is shown in Fig. 2. Two stainless steel heat pipes with quartz windows at the ends and filled with lead-noble gas (Ar, He) mixture were used in the measurements. Noble gas pressure in one heat pipe (reference) was kept at constant pressure (p_0=25 mbar), while in the second one (henceforth called "working") it was varied in the range from 25 to

* Corresponding author. Fax: +385 1 469 8889.
E-mail address: blecic@ifs.hr (V. Horvatic).

0584-8547/$ – see front matter © 2008 Elsevier B.V. All rights reserved.
doi:10.1016/j.sab.2008.04.003

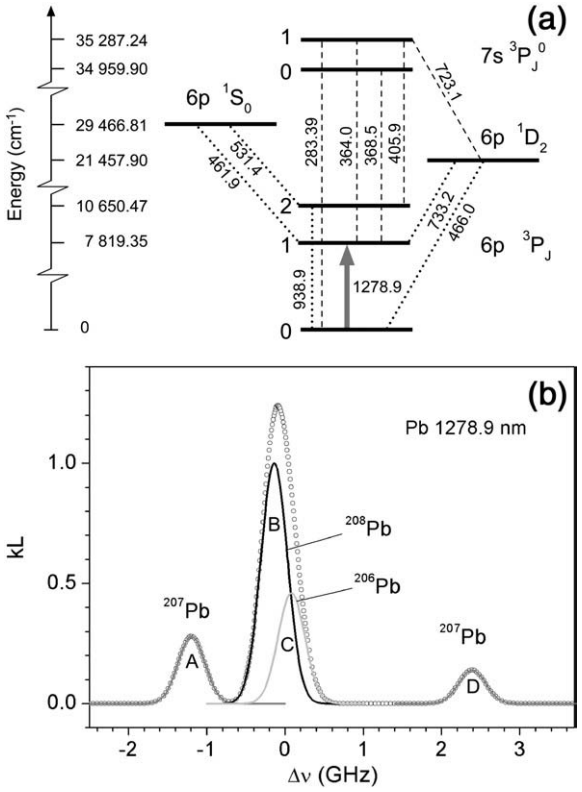

Fig. 1. (a) Partial term diagram of lead. The numbers associated with dashed and dotted lines are the transition wavelengths in nanometers. The solid arrow indicates the forbidden transition at 1278.9 nm investigated in the present experiment. The dotted lines indicate dipole forbidden transitions. (b) The structure of the 1278.9 nm line for natural abundant lead (^{208}Pb: 52%, ^{207}Pb: 22%, ^{206}Pb: 25%, ^{204}Pb: ≈1%) with contributions to optical depth kL arising from different isotopes: ^{207}Pb (lines A and D), ^{208}Pb (line B) and ^{206}Pb (line C). Very weak contribution due to ^{204}Pb isotope is not included. The relative strengths of the components are proportional to the respective abundances. Intensities of the hyperfine components (F=1/2, 3/2) of the ^{207}Pb $^3P_1$ states are in the ratio 2:1. The solid lines represent Doppler profiles of the Pb isotopes calculated for T=1200 K. The envelope of the line is indicated with open symbols. The values for isotope shifts and the hyperfine splitting for the ^{207}Pb isotope are taken from [19].

500 mbar. The heat pipes were operated in a hot-pipe regime. The lead vapor was generated by outer resistive heating of the central part of the hot-pipe oven, where a high-purity natural abundant lead (^{208}Pb: 52%, ^{207}Pb: 22%, ^{206}Pb: 25%, ^{204}Pb: ≈1%), was placed. Both hot-pipes had heated zones of the same length. With a help of very thin tungsten wire built-in along the hot-pipe axis, which was dismounted after being exposed to a heating-cooling cycle, the effective vapor column length L=(4±0.5) cm was determined from the length of the segment on which the lead was deposited. The Pb number densities in both hot-pipes were adjusted to be equal by varying their heating currents until the same peak absorption at the strongest spectral feature was produced under the same initial pressure conditions (p=p_0=25 mbar).

In the way previously described [7], the temperature of the vapor and lead number density were determined by the measurements of the equivalent width of the optically thick lead resonance line at 283.4 nm ($6p^2\ ^3P^0 \rightarrow 7s$ transition) and using the lead vapor pressure curve given by Nesmeyanov [20]. The resonance absorption was measured using the continuum of a deuterium lamp and a 0.5 m Jarrel–Ash monochromator (spectral resolution: 0.03 nm) with an RCA 1P28 photomultiplier. The measurements were performed under the following lead number density and temperature conditions: N_{Pb}=(4.8±1.5)×10^{15} cm^{-3}; T=(1220±25) K and N_{Pb}=(1.2±0.4)×10^{16} cm^{-3}; T=(1290±25) K, in argon and helium, respectively. The measurements in Ar and He have been made at slightly different temperatures in order to produce the absorption spectra of the same quality at high noble gas pressures. Namely, He caused slightly stronger broadening, and these measurements were made at slightly higher Pb number density to ensure the peak absorption at high noble gas pressure comparable to the one in Ar.

A single-mode DFB diode laser (Laser Components, type SPECDILAS D-Series, line width: 10 MHz, side mode suppression: 25 dB) was used to measure the absorption at $6p^2\ ^3P_0 \rightarrow 6p^2\ ^3P_1$ transition. Current and temperature of the laser diode were controlled by commercial driver (PROFILE Optische Systeme GmbH, model ITC 502). Laser beam was split into three parts. One very weak part was directed to a confocal Fabry–Perot interferometer (FPI) with 2 GHz free spectral range, which was used for wavelength calibration of the absorption spectra. The other two parts of the beam were transmitted through the hot-pipe ovens. The power of the beams directed through the hot pipes was reduced by neutral density filters to ~500 μW in order to avoid saturation of the photodetectors. The transmitted laser intensities (through hot pipes and FPI) were detected by a near-infrared photodiodes: PbS (Hamamatsu, P9217) and InGaAs PIN (Hamamatsu, G8370). The laser beam was mechanically chopped, the measured intensity signals amplified by Lock-In amplifiers (Stanford Research model 510, EG&G PAR model 5210), and the outputs fed to a laboratory PC. The data were collected using LabView program, and stored on the computer for later analysis.

The laser scan over the $6p^2\ ^3P_0 \rightarrow 6p^2\ ^3P_1$ transition was made by tuning the current of the laser diode at a fixed temperature. The laser frequency was scanned up and down, and the transmitted intensities of the FPI and the hot pipes were recorded simultaneously. An example of the obtained spectra is shown in Fig. 3. The actual width of the scan (typical scan range: about 50 GHz) was much larger than displayed in Fig. 3. This procedure ensured that the scan in the region of the Pb line was free of small, non-linearity observed at the very ends (2–4 GHz wide interval) of the scan where the laser sweep reversed direction.

3. Measurements and results

The frequency dependent absorption coefficient of the medium $k(\nu)$ is given by the following relation:

$$k(\nu) = K\,N\,P(\nu - \nu_{12}), \tag{1}$$

where K is defined by the well-known Ladenburg relation [21]:

$$K = \frac{\pi e^2}{m_e c} f_{12} = \frac{g_2}{g_1}\frac{c^2}{8\pi\nu_{12}^2} A_{21}. \tag{2}$$

In the above expressions, $P(\nu-\nu_0)$ [Hz^{-1}] is the normalized ($\int P d\nu = 1$) line profile, ν_{12} is the central frequency of the $1 \rightarrow 2$ transition, f_{12} is the line oscillator strength, and e and m_e are the electron charge and mass, respectively. The spontaneous radiative rate is labeled with A_{21}, while g_1 and g_2 are the statistical weights of the lower and upper levels, respectively. The ground state atom number density is denoted by N.

The Pb 1278.9 nm line was measured in the impact region where, according to the Lindholm theory [22], the profile of the single homogeneously broadened line has a Lorentzian shape. In its normalized form, Lorentzian line profile reads:

$$P_L(\nu - \nu_{12}) = \frac{1}{2\pi}\frac{\Gamma_B}{(\nu_{12} - \nu + \Gamma_S)^2 + (\Gamma_B/2)^2}, \tag{3}$$

were Γ_B and Γ_S are the line broadening and shift rates, respectively, expressed in units s^{-1}. The Γ_B represents the line full width at half maximum (FWHM). The rates Γ_B and Γ_S can be expressed as:

$$\Gamma_B = \Gamma_{nat} + \Gamma_{coll} = \Gamma_{nat} + \gamma_B \times N_P, \tag{4}$$

$$\Gamma_S = \gamma_S \times N_P, \tag{5}$$

where Γ_{nat} is the natural broadening rate, γ_B and γ_S are the collisional broadening and shift rate coefficients, and N_P is the number density of the perturber causing the spectral line broadening and shift.

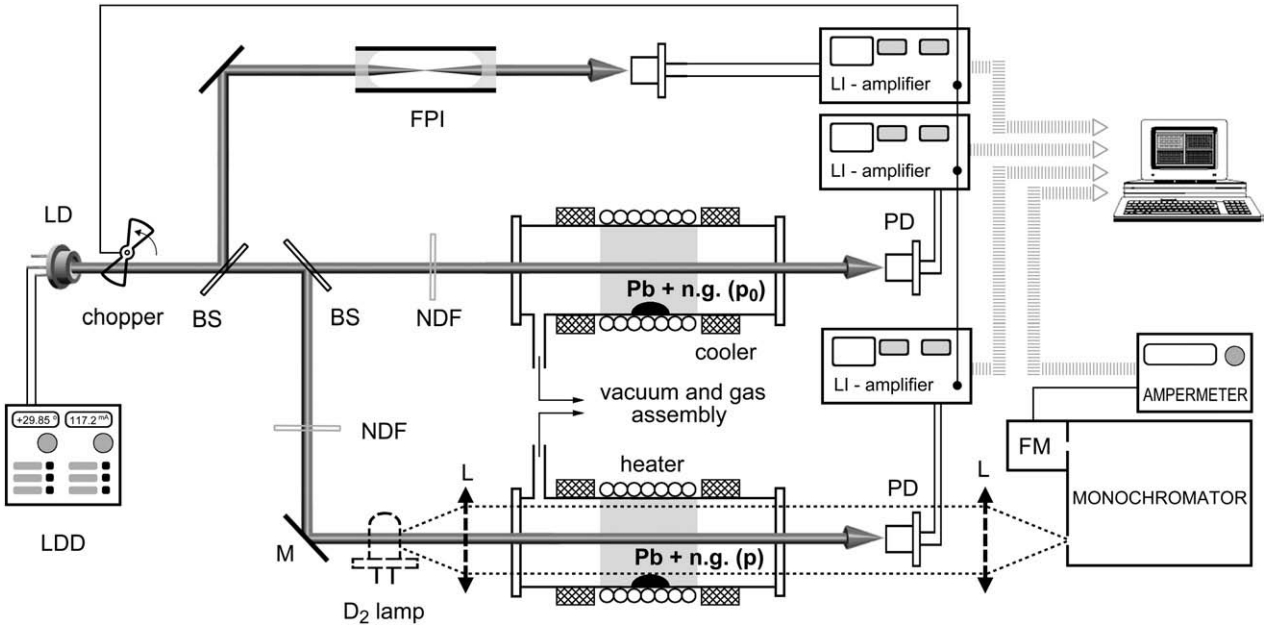

Fig. 2. Experimental setup used in the measurements of Ar- and He-induced broadening and shift of the Pb 1278.9 nm line. LD — laser diode, LDD — laser diode driver, FPI — Fabry–Perot interferometer, M — mirror, BS — beam splitter, NDF — natural density filter, L — lens, PD — photodiode, FM — photomultiplier, (Pb+n.g) — lead-noble gas mixture at reference (p_0) and variable (p) noble gas pressure.

The shape of the measured hyperfine and isotope components of the Pb 1278.9 nm line were of the Voigt type, i.e., the convolution of a Gaussian (Doppler broadening) and Lorentzian profile (natural and collisional broadening). The normalized Voigt profile of a single line is given by [23]:

$$P_V(\nu,a)=\frac{1}{2\pi^{3/2}\Delta_G}\int_{-\infty}^{+\infty}\exp(-x^2)\frac{a}{\left(\frac{\nu-\nu_{12}}{\Delta_G}-\frac{x}{2\sqrt{\ln 2}}\right)^2+\left(\frac{a}{2}\right)^2}dx, \quad (6)$$

where $a=\Gamma_B/\Delta_G$ is the Voigt parameter, with $\Delta_G=2(\ln 2)^{1/2}(\nu_{12}/c)(2k_BT/M)^{1/2}$ denoting the Doppler width of the profile. In the latter expression T is the temperature, while k_B and M are the Boltzmann constant and the mass of the atom, respectively. The variable of integration is $x=v_x/v_m$, where $v_x=(c/\nu_{12})(\nu-\nu_{12})$ and $v_m=(2k_BT/M)^{1/2}$ is the Maxwellian most probable velocity.

The absorption profile $k(\nu)$ of the measured lead line is a composition of several hyperfine and isotope components, where each one exhibits the Voigt form. Therefore, the total Voigt profile can be represented by:

$$P_V^{tot}(\nu,a)=\frac{1}{2\pi^{3/2}\Delta_G}\sum_i S_i\int_{-\infty}^{+\infty}\exp(-x^2)\frac{a}{\left(\frac{\nu-\nu_{12}^i}{\Delta_G}-\frac{x}{2\sqrt{\ln 2}}\right)^2+\left(\frac{a}{2}\right)^2}dx, \quad (7)$$

where index i=A, B, C, D counts different isotope and hyperfine components (see Fig. 1). The central frequencies ν_{12}^i of the components were calculated relative to the center of gravity of the ^{207}Pb hyperfine lines. The values of the isotope and hyperfine splitting were taken from [19]. The S_i label relative strengths of the components of the 1278.9 nm line (S_A: S_B: S_C: S_D=0.28: 1: 0.46: 0.14) which are proportional to the respective abundances of the Pb isotopes, where the strength of the ^{207}Pb line is split in 2:1 ratio between its hyperfine components. The Doppler width Δ_G was calculated using the temperature determined in the experiment, as described in Section 2. Note that different to $P_V(\nu, a)$ for a single line (Eq. (6)), the profile $P_V^{tot}(\nu, a)$ is not normalized.

The theoretical $P_V^{tot}(\nu, a)$ profiles for a series of a-parameters in the range relevant for the comparison with the measured spectra, were calculated using the program Mathcad 2001 Professional.

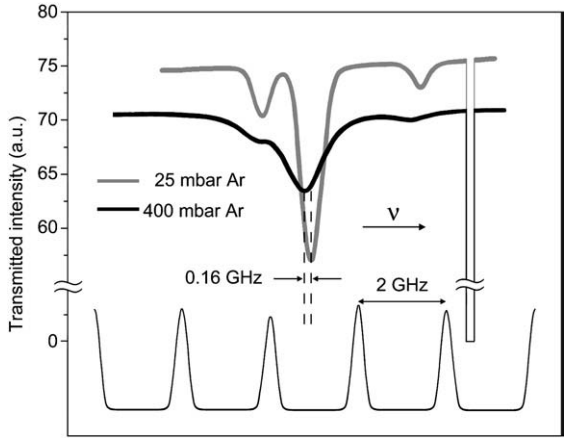

Fig. 3. Example of the simultaneous absorption scans taken in the reference heat pipe (p_0=25 mbar) and the heat pipe with variable Ar pressure. Bottom trace represents the transmission peaks of the Fabry–Perot interferometer with f.s.r of 2 GHz.

3.1. Determination of the broadening rates

In the present measurements the laser line width (Δ_{las}=10 MHz) was always at least 60 times (at low noble gas pressure) narrower than the width of the investigated line profiles. Therefore, the shape of the absorption coefficient $k(\nu)$ could be correctly determined.

It is known that in the infrared and microwave region, collisions may sometimes cause a narrowing (Dicke narrowing) instead of a broadening of the line. When the Doppler width is larger than the pressure-broadened width, Dicke narrowing can occur if the mean free path is smaller than the wavelength of the transition. In the range of noble gas pressures 25 mbar$<p<$450 mbar relevant for the present experiment, the mean free path l in Pb–Ar and Pb–He collisions could be estimated to be in the range 30 μm$>l>$2 μm and 44 μm$>l>$3 μm, respectively. In the case at hand, the Doppler width exceeded the Lorentzian width ($a<1$) up to the pressures of ~200 mbar, but in that range the corresponding mean free path was 3–23 (for Ar) or 5–34 (for

He) times larger than the wavelength of the investigated transition. Therefore the effect of Dicke narrowing in the present experiment can be neglected.

The laser light intensities transmitted through the two heat pipes were recorded simultaneously with the dispersion calibration marks of the FPI, while scanning the laser across 1278.9 nm line. The measurements were made for a series of noble gas (Ar, He) pressures in the working heat pipe that were in the range from 25 to 500 mbar. The noble gas pressure in the reference heat pipe was kept constant at p_0=25 mbar. In this part of the measurements the signal of the reference heat pipe, exhibiting narrow and well resolved lines, served only as an additional control of the spectrum dispersion and the linearity of the laser scan. At each noble gas pressure the absorption coefficient was evaluated as $k(\nu)=(1/L)\times\ln[I_0(\nu)/I(\nu)]$, where $I(\nu)$ and $I_0(\nu)$ were the transmitted and incident light intensities, respectively, while L was the length of the absorbing vapor column.

At the maximum Pb number density $\sim 1.2\times10^{16}$ cm^{-3} and temperature of ~1290 K in the experiment, the lead pressure amounted to 1.2 mbar, which was more than one order of magnitude lower than the lowest noble gas pressure used in the measurements. In other words, the pressure in the hot zone could be entirely attributed to the noble gas, and the corresponding number density was determined from the total pressure p measured by manometer and temperature T of the vapor by using the ideal gas law, i.e., $N_{ng}=p/k_BT$.

In order to fit the measured $k(\nu)$ into the field of the theoretical Voigt profiles, both the $k(\nu)$ and the Voigt profiles given by Eq. (7) were normalized to unity at the central frequency of the strongest spectral component (peak of ^{206}Pb and ^{208}Pb envelope). The experimental $k(\nu)/k_0(\nu_0)$ data (k_0 and ν_0 label the peak value and the frequency of strongest component of 1278.9 nm line) were inserted into the field of calculated Voigt profiles and the parameter a corresponding to the measured spectrum was determined. The illustration of this procedure is given in Fig. 4 for the case of Ar as a perturber. The examples are given for the lowest and highest investigated Ar pressure. In this way the Voigt parameter a could be determined with an error of at most ±0.1. In the case of He as a perturber the results similar to those displayed in Fig. 4. were obtained.

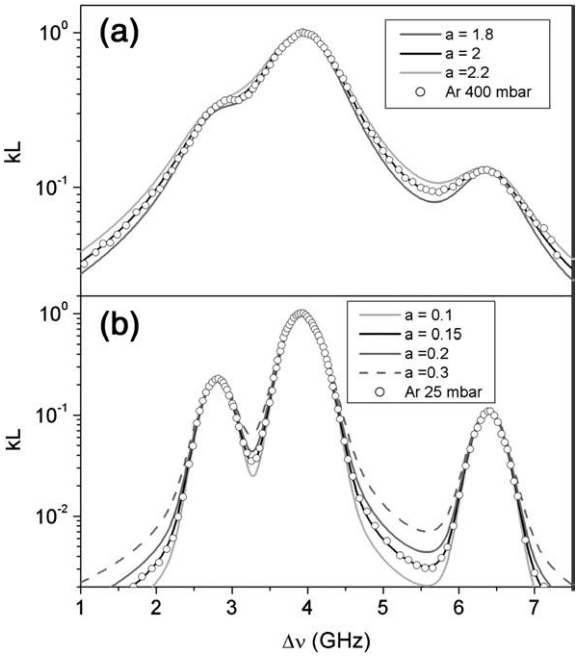

Fig. 4. Fitting of the measured normalized optical depths kL of the 1278.9 nm line into the field of the Voigt profiles calculated (see text for details) for a series of a-values. Both the experimental data and the calculated Voigt profiles were normalized to unity at the central frequency ν_0 of the strongest spectral component (^{206}Pb and ^{208}Pb envelope, having the peak value k_0), and plotted as functions of relative detuning $\Delta\nu=\nu-\nu_0$. Examples are displayed for Ar as the perturber at two pressures typical for the region of (a) high, and (b) low pressures.

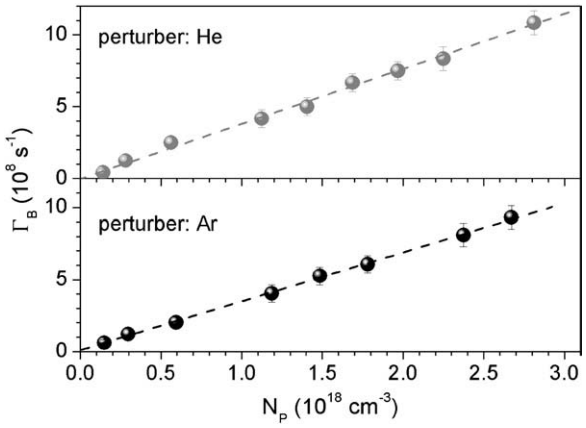

Fig. 5. Broadening rates Γ_B of the Pb 1278.9 nm line in dependence on the perturber number density N_P (P=Ar, He). Ar- and He-induced broadenings were measured at 1220 K and 1290 K, respectively. The dashed straight lines represent least squares fits to the measured data, yielding $\gamma_B^{Ar}=(3.4\pm0.1)\times10^{-10}$ cm^3 s^{-1} and $\gamma_B^{He}=(3.8\pm0.1)\times10^{-10}$ cm^3 s^{-1}.

From the a values obtained in dependence on the noble gas number density and calculated Doppler width, the Lorentzian width Γ_B was obtained as a function of N_{ng}. The results for Ar and He as a perturber are displayed in Fig. 5. The depicted error bars include uncertainty due to inaccuracy in the Voigt parameter a and the Doppler width Δ_G (i.e. vapor temperature T). The slope of the least squares fit through the experimental points, yielded the following values for the collisional broadening rate coefficients of the Pb forbidden line at 1278.9 nm:

$$\gamma_B^{Ar}=(3.4\pm0.1)\times10^{-10}\text{cm}^3\,\text{s}^{-1}, \quad (8)$$

$$\gamma_B^{He}=(3.8\pm0.1)\times10^{-10}\text{cm}^3\,\text{s}^{-1}. \quad (9)$$

The declared error represents the statistical error of the least square fit through the data weighted by the experimental error bars. The intercept of the fitted straight line, which represents the value of Γ_{nat}, is zero within the limits of the error bar. This is accordance with the result for the radiative transition probability of this transition [7] which yielded $\Gamma_{nat}=0.97$ s^{-1}.

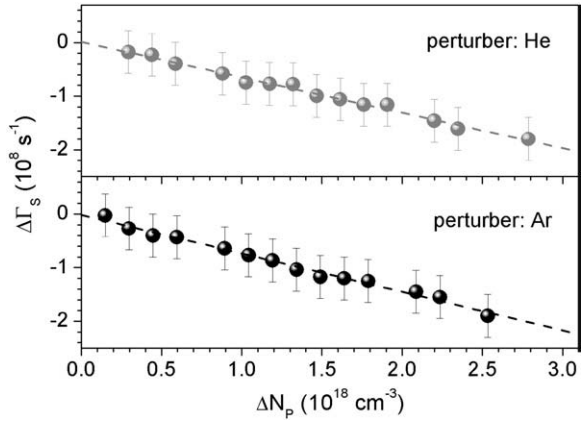

Fig. 6. The shift rate difference $\Delta\Gamma_S$ of the 1278.9 nm line in dependence on the perturber density difference ΔN_P (see text for explanation). The measurements in Ar and He were carried out at T=1220 K and T=1290 K, respectively. The dashed straight lines are least squares fits to the experimental points, yielding $\gamma_S^{Ar}=(-7.3\pm0.8)\times10^{-11}$ cm^3 s^{-1} and $\gamma_S^{He}=(-6.5\pm0.7)\times10^{-11}$ cm^3 s^{-1}.

3.2. Determination of shift rates

The shifts of the 1278.9 nm line due to Ar and He were determined from the simultaneous measurements in the reference (noble gas pressure p_0=25 mbar) heat pipe and the heat pipe with variable noble gas pressure p. The position of the peak of the strongest component (^{206}Pb and ^{208}Pb envelope) at pressure p was measured relative to its position at reference pressure p_0. The dispersion was determined by the transmission peaks of the Fabry–Perot interferometer (f.s.r.: 2 GHz). The measured line shift differences $\Delta\Gamma_S$ in dependence on the perturber number density differences $\Delta N_P = N_P(p) - N_P(p_0)$ are plotted in Fig. 6. The slope of the straight line $\Delta\Gamma_S$ vs. ΔN_P obtained by least square fit through the experimental points weighted by the error bars, yielded the following collisional shift rate coefficients for Ar and He:

$$\gamma_S^{Ar} = (-7.3 \pm 0.8) \times 10^{-11} \mathrm{cm}^3\,\mathrm{s}^{-1}, \quad (10)$$

$$\gamma_S^{He} = (-6.5 \pm 0.7) \times 10^{-11} \mathrm{cm}^3\,\mathrm{s}^{-1}. \quad (11)$$

The declared error represents the statistical error of the least square fits.

As can be seen in Fig. 6 both Ar and He cause small red shifts.

4. Discussion and conclusion

The present results complete the set of broadening and shift data [15,18] for the lines occurring in the transitions among $6p^2\ ^3P_0$, $6p^2\ ^3P_J$ (J=1, 2) and $7s\ ^3P_J^0$ (J=0, 1) states of lead, induced by collisions with Ar and He.

As shown in Section 3, Ar and He cause similar broadening of the Pb 1278.9 nm line. Moreover, both perturbers shift the line towards red. In the case of He this is rather rare case [3] and points to an intricate balance between attractive and repulsive parts of the potentials involved.

In absence of high quality *ab initio* Pb-noble gas potentials, one might speculate upon the type of the interaction responsible for the investigated broadening and shift of the Pb 1278.9 nm line. Even in the case of commonly adopted Lennard–Jones potentials the simple inversion procedure for obtaining the potentials from the experimental data leads to ambiguous results [3], which call for some additional data in order to reach the final conclusion. Therefore at this stage of research we did not attempt to extract Pb-noble gas long-range difference interaction potentials from the broadening and shift data.

To summarize, the broadening and shift of the "forbidden" Pb line at 1278.9 nm lead have been measured due to the presence of the noble gases Ar and He. The results for the broadening and shift constants were obtained from simultaneous diode laser absorption measurements in two hot-pipes, out of which one was kept at low noble gas pressure and served as a reference, while in the other one noble gas pressure was varied. The shift rates were obtained by measuring the position of the strongest absorption peak of the 1278.9 nm line relative to its position recorded in the reference hot-pipe spectrum. The broadening rates were determined by fitting the measured line shapes to theoretical Voigt profiles. The measurements carried out at T=1220 K (in Ar) and T=1290 K (in He), i.e. at lead number densities of 4.8×10^{15} cm^{-3} and 1.2×10^{16} cm^{-3}, respectively, yielded the following broadening and shift constants: $\gamma_B^{Ar}=(3.4\pm0.1)\times10^{-10}$ cm^3 s^{-1}, $\gamma_B^{He}=(3.8\pm0.1)\times10^{-10}$ cm^3 s^{-1}, $\gamma_S^{Ar}=(-7.3\pm0.8)\times10^{-11}$ cm^3 s^{-1}, $\gamma_S^{He}=(-6.5\pm0.7)\times10^{-11}$ cm^3 s^{-1}.

Acknowledgements

The presented investigations were obtained within the frame of the project No. 035-0352851-2853 finacially suported by the Ministry of Science, Education and Sports of the Republic of Croatia. Funding by the Deutsche Forschungsgemeinschaft (DFG, project KRO 113/00) is gratefully acknowledged. The authors also thank the Ministry of Innovation, Science, Research and Technology of the state Northrhine-Westphalia and the Ministry of Education and Research of the Federal Republic of Germany for general support.

References

[1] H. Margenau, W.W. Watson, Pressure effects on spectral lines, Rev. Mod. Phys. 8 (1936) 22–53.
[2] S.Y. Ch'en, M. Takeo, Broadening and shift of spectral lines due to the presence of foreign gases, Rev. Mod. Phys. 29 (1957) 20–73.
[3] N. Allard, J. Kielkopf, The effect of neutral nonresonant collisions on atomic spectral lines, Rev. Mod. Phys. 54 (1982) 1103–1182.
[4] A. Unsöld, The New Cosmos, Springer-Verlag, Berlin, 1977, p. 169.
[5] J. Weiner, V.S. Bagnato, S. Zilio, P.S. Julienne, Experiments and theory in cold and ultracold collisions, Rev. Mod. Phys. 71 (1999) 1–85.
[6] J.A. Gelbwachs, Atomic resonance filters, IEEE J. Quantum Electron. 24 (1988) 1266–1277.
[7] C. Vadla, V. Horvatic, K. Niemax, Oscillator strength of the strongly "forbidden" Pb $6p^2\ ^3P_0 \rightarrow 6p^2\ ^3P_1$ transition at 1278.9 nm, Eur. Phys. J. D 14 (2001) 23–25.
[8] V. Horvatic, C. Vadla, M. Movre, The collision cross sections for excitation energy transfer in $Rb^*(5P_{3/2})+K(4S_{1/2}) \leftrightarrow Rb(5S_{1/2})+K^*(4P_J)$ processes, Z. Phys. D 27 (1993) 123–130.
[9] V. Horvatic, D. Veza, M. Movre, K. Niemax, C. Vadla, Collision cross sections for excitation energy transfer in $Na^*(3P_{1/2})+K(4S_{1/2}) \leftrightarrow Na^*(3P_{3/2})+K(4S_{1/2})$ processes, Z. Phys. D 34 (1995) 163–170.
[10] C. Vadla, V. Horvatic, The $6s5d\ ^1D_2 \rightarrow 6s5d\ ^3D_J$ excitation energy transfer in barium induced by collisions with He, Ar and Xe atoms, FIZIKA A 4 (1995) 463–472.
[11] V. Horvatic, C. Vadla, M. Movre, K. Niemax, The collision cross sections for the fine-structure mixing of caesium 6P levels induced by collisions with potassium atoms, Z. Phys. D 36 (1996) 101–104.
[12] T.L. Correll, V. Horvatic, N. Omenetto, C. Vadla, J.D. Winefordner, Quantum efficiency improvement of a cesium based resonance fluorescence detector by helium-induced collisional excitation energy transfer, Spectrochim. Acta Part B 60 (2005) 765–774.
[13] T.L. Correll, V. Horvatic, N. Omenetto, J.D. Winefordner, C. Vadla, Experimental evaluation of the cross sections for the $Cs(6D) \rightarrow Cs(7P_J)$ and $Cs(6D_{5/2}) \rightarrow Cs(6D_{3/2})$ collisional transfer processes induced by He and Ar, Spectrochim. Acta Part B 61 (2006) 623–633.
[14] C. Vadla, V. Horvatic, K. Niemax, Energy pooling to the Ba $6s6p\ ^1P^0_1$ level arising from collisions between pairs of metastable Ba $6s5d\ ^3D_J$ atoms, Eur. Phys. J. D 1 (1998) 139–147.
[15] J. Franzke, H.D. Wizemann, K. Niemax, C. Vadla, Impact broadening and shift rates for the $6p^2\ ^3P_{J'} \rightarrow 7s\ ^3P^0_J$ transitions of lead induced by collisions with argon and helium, Eur. Phys. J. D 8 (2000) 23–28.
[16] C. Vadla, M. Movre, R. Beuc, J. Franzke, H.-D. Wizemann, K. Niemax, Optimization of lead metastable production in a low pressure argon discharge, Spectrochim. Acta Part B 55 (2000) 1759–1769.
[17] J.R. Fuhr, A. Lesage, Bibliography on Atomic Line Shapes and Shifts, NIST Special Publication, vol. 366, U.S. Government Printing Office, Washington D.C., 1994.
[18] M. Kotteritzsch, W. Gries, A. Hese, Foreign gas broadening and shift in the lead resonance line at λ=283.3 nm, J. Phys. B: At., Mol. Opt. Phys. 25 (1992) 913–922.
[19] J.M. Reeves, E.N. Fortson, Isotope shifts at 1.28 μm in Pb, Phys. Rev. A 44 (1991) R1439–R1441.
[20] A.N. Nesmeyanov, Vapor pressure of elements, Academic, New York, 1963.
[21] R. Ladenburg, Die quantentheoretische Zahl der Dispersionselektronen, Z. Phys. 4 (1921) 451–468.
[22] E. Lindholm, Über die Verbreiterung und Verschiebung von Spektrallinien, Dissertation, Uppsala 1942.
[23] A.C.G. Mitchell, M.W. Zemansky, Resonance Radiation and Excited Atoms, University Press, Cambridge, 1971.